

hep-ph/9312296
 CERN-TH.7057/93
 IEM-FT-81/93
 FTUAM-36/93

Aspects of the electroweak phase transition in the Minimal Supersymmetric Standard Model¹

A. Brignole²,

Dep. de Física Teórica, Universidad Autónoma de Madrid
 Cantoblanco, E-28049 Madrid, Spain

J.R. Espinosa³, M. Quirós⁴

Instituto de Estructura de la Materia, CSIC
 Serrano 123, E-28006 Madrid, Spain

and

F. Zwirner⁵

Theory Division, CERN
 CH-1211 Geneva 23, Switzerland

Abstract

We study the finite-temperature effective potential of the Minimal Supersymmetric Standard Model in the full $(m_A, \tan \beta)$ parameter space. As for the features of the electroweak phase transition, we identify two possible sources of significant differences with respect to the Standard Model: a stop sector with little supersymmetry breaking makes the phase transition more strongly first-order, whereas a light CP-odd neutral boson weakens its first-order nature. After including the leading plasma effects, $T = 0$ radiative corrections due to top and stop loops, and the most important experimental constraints, we find that the danger of washing out any baryon asymmetry created at the electroweak scale is in general no less than in the Standard Model.

CERN-TH.7057/93

December 1993

¹Work supported in part by the European Union under contract No. CHRX-CT92-0004.

²Supported by a postdoctoral fellowship of the Ministerio de Educación y Ciencia, Spain. Address after November 7, 1993: Theory Group, Lawrence Berkeley Laboratory, Berkeley CA 94720, USA.

³Supported by a grant of Comunidad de Madrid, Spain.

⁴Work partly supported by CICYT, Spain, under contract AEN93-0139.

⁵On leave from INFN, Sezione di Padova, Padua, Italy.

1. The option of generating the cosmological baryon asymmetry at the electroweak phase transition is not necessarily the one chosen by Nature, but it is certainly fascinating, and has recently deserved a lot of attention [1]. At the qualitative level, the Standard Model (SM) meets the basic requirements for a successful implementation of this scenario. At the quantitative level, however, it suffers from two basic problems. First, the amount of CP violation in the Kobayashi-Maskawa matrix appears to be insufficient, even after taking into account the large uncertainties associated with dynamical models of baryogenesis¹. Secondly, one must make sure that sphaleron interactions in the broken phase do not wash out, at the completion of the phase transition, any previously created baryon asymmetry. This requirement suggests that the transition should be rather strongly first order, $v(T_C)/T_C \gtrsim 1$, where T_C is the critical temperature and $v(T_C)$ is the symmetry-breaking vacuum expectation value. In the SM, this condition turns out to be incompatible with the experimental limits [4] on the Higgs mass, $m_\phi > 63.5$ GeV at 95% c.l., even after implementing the conventional techniques for dealing with the infrared problem [1,5]. To cure both problems, one can consider plausible extensions of the SM, to see if they can allow for additional sources of CP violation and for an enhanced strength of the first-order phase transition. Among these extensions, the physically most motivated and phenomenologically most acceptable one is the Minimal Supersymmetric Standard Model (MSSM). This model allows for extra CP-violating phases besides the Kobayashi-Maskawa one, which could help in generating the observed baryon asymmetry [6]. It is then interesting to study whether in the MSSM the nature of the phase transition can be significantly modified with respect to the SM.

In a recent paper [7], some of us have considered the MSSM in the limit $m_A \rightarrow \infty$, corresponding to only one light Higgs with SM properties, and improved over previous studies [8] by including a full discussion of the top/stop sector, and by resumming the leading plasma corrections to gauge boson and stop masses. It was found that this special limit of the MSSM can only marginally improve the situation with respect to the SM case. In the present paper, we extend the considerations of [7] to the full $(m_A, \tan \beta)$ parameter space, characterizing the Higgs sector of the MSSM. Even barring the interesting possibility of spontaneous CP-violation at finite temperature [9], as well as the possibility of charge- and colour-breaking minima, we have to deal with a complicated two-variable potential, which requires a numerical analysis. However, to allow for an understanding of the behaviour of various quantities, we also produce some approximate analytical formulae. After including the most important experimental constraints, we find that there is very little room for the MSSM to improve over the SM.

2. The main tool for our study is the one-loop, daisy-improved finite-temperature effective potential of the MSSM, $V_{\text{eff}}(\phi, T)$. We are actually interested in the dependence of the potential on $\phi_1 \equiv \text{Re } H_1^0$ and $\phi_2 \equiv \text{Re } H_2^0$ only, where H_1^0 and H_2^0 are the neutral

¹Unorthodox views on this point, recently put forward in [2], have been subsequently questioned in [3].

components of the Higgs doublets H_1 and H_2 , thus ϕ will stand for (ϕ_1, ϕ_2) . Working in the 't Hooft-Landau gauge and in the \overline{DR} -scheme, we can write

$$V_{\text{eff}}(\phi, T) = V_0(\phi) + V_1(\phi, 0) + \Delta V_1(\phi, T) + \Delta V_{\text{daisy}}(\phi, T), \quad (1)$$

where

$$V_0(\phi) = m_1^2 \phi_1^2 + m_2^2 \phi_2^2 + 2m_3^2 \phi_1 \phi_2 + \frac{g^2 + g'^2}{8} (\phi_1^2 - \phi_2^2)^2, \quad (2)$$

$$V_1(\phi, 0) = \sum_i \frac{n_i}{64\pi^2} m_i^4(\phi) \left[\log \frac{m_i^2(\phi)}{Q^2} - \frac{3}{2} \right], \quad (3)$$

$$\Delta V_1(\phi, T) = \frac{T^4}{2\pi^2} \left\{ \sum_i n_i J_i \left[\frac{m_i^2(\phi)}{T^2} \right] \right\}, \quad (4)$$

$$\Delta V_{\text{daisy}}(\phi, T) = -\frac{T}{12\pi} \sum_i n_i [\bar{m}_i^3(\phi, T) - m_i^3(\phi)]. \quad (5)$$

The four contributions (2–5) to the effective potential (1) have the following meaning. The first term, eq. (2), is the tree-level potential. The second term, eq. (3), is the one-loop contribution at $T = 0$: Q is the renormalization scale, where we choose for definiteness $Q^2 = m_Z^2$, $m_i^2(\phi)$ is the field-dependent mass of the i^{th} particle, and n_i is the corresponding number of degrees of freedom, taken negative for fermions. Since $V_1(\phi, 0)$ is dominated by top (t) and stop (\tilde{t}_1, \tilde{t}_2) contributions, only these will be included in the following. The third term, eq. (4), is the additional one-loop contribution due to temperature effects. Here $J_i = J_+(J_-)$ if the i^{th} particle is a boson (fermion), and

$$J_{\pm}(y^2) \equiv \int_0^\infty dx x^2 \log \left(1 \mp e^{-\sqrt{x^2+y^2}} \right). \quad (6)$$

Since the relevant contributions to $\Delta V_1(\phi, T)$ are due to top (t), stops (\tilde{t}_1, \tilde{t}_2) and gauge bosons (W, Z), only these will be considered in the following. Finally, the last term, eq. (5), is a correction coming from the resummation of the leading infrared-dominated higher-loop contributions, associated with the so-called daisy diagrams. The sum runs over bosons only. The masses $\bar{m}_i^2(\phi, T)$ are obtained from the $m_i^2(\phi)$ by adding the leading T -dependent self-energy contributions, which are proportional to T^2 . We recall that, in the gauge boson sector, only the longitudinal components (W_L, Z_L, γ_L) receive such contributions.

The relevant degrees of freedom for our calculation are:

$$n_t = -12, \quad n_{\tilde{t}_1} = n_{\tilde{t}_2} = 6, \quad n_W = 6, \quad n_Z = 3, \quad n_{W_L} = 2, \quad n_{Z_L} = n_{\gamma_L} = 1. \quad (7)$$

The field-dependent top mass is

$$m_t^2(\phi) = h_t^2 \phi_2^2. \quad (8)$$

The entries of the field-dependent stop mass matrix are

$$m_{\tilde{t}_L}^2(\phi) = m_{Q_3}^2 + m_t^2(\phi) + D_{\tilde{t}_L}^2(\phi), \quad (9)$$

$$m_{\tilde{t}_R}^2(\phi) = m_{U_3}^2 + m_t^2(\phi) + D_{\tilde{t}_R}^2(\phi), \quad (10)$$

$$m_X^2(\phi) = h_t(A_t \phi_2 + \mu \phi_1), \quad (11)$$

where m_{Q_3} , m_{U_3} and A_t are soft supersymmetry-breaking mass parameters, μ is a super-potential Higgs mass term, and

$$D_{\tilde{t}_L}^2(\phi) = \left(\frac{1}{2} - \frac{2}{3} \sin^2 \theta_W\right) \frac{g^2 + g'^2}{2} (\phi_1^2 - \phi_2^2), \quad (12)$$

$$D_{\tilde{t}_R}^2(\phi) = \left(\frac{2}{3} \sin^2 \theta_W\right) \frac{g^2 + g'^2}{2} (\phi_1^2 - \phi_2^2) \quad (13)$$

are the D -term contributions. The field-dependent stop masses are then

$$m_{\tilde{t}_{1,2}}^2(\phi) = \frac{m_{\tilde{t}_L}^2(\phi) + m_{\tilde{t}_R}^2(\phi)}{2} \pm \sqrt{\left[\frac{m_{\tilde{t}_L}^2(\phi) - m_{\tilde{t}_R}^2(\phi)}{2}\right]^2 + [m_X^2(\phi)]^2}. \quad (14)$$

The corresponding effective T -dependent masses, $\overline{m}_{\tilde{t}_{1,2}}^2(\phi, T)$, are given by expressions identical to (14), apart from the replacement

$$m_{\tilde{t}_{L,R}}^2(\phi) \rightarrow \overline{m}_{\tilde{t}_{L,R}}^2(\phi, T) \equiv m_{\tilde{t}_{L,R}}^2(\phi) + \Pi_{\tilde{t}_{L,R}}(T). \quad (15)$$

The $\Pi_{\tilde{t}_{L,R}}(T)$ are the leading parts of the T -dependent self-energies of $\tilde{t}_{L,R}$,

$$\Pi_{\tilde{t}_L}(T) = \frac{4}{9} g_s^2 T^2 + \frac{1}{4} g^2 T^2 + \frac{1}{108} g'^2 T^2 + \frac{1}{6} h_t^2 T^2, \quad (16)$$

$$\Pi_{\tilde{t}_R}(T) = \frac{4}{9} g_s^2 T^2 + \frac{4}{27} g'^2 T^2 + \frac{1}{3} h_t^2 T^2, \quad (17)$$

where g_s is the strong gauge coupling constant. Only loops of gauge bosons, Higgs bosons and third generation squarks have been included, implicitly assuming that all remaining supersymmetric particles are heavy and decouple. If some of these are also light, the plasma masses for the stops will be even larger, further suppressing the effects of the associated cubic terms, and therefore weakening the first-order nature of the phase transition. Finally, the field-dependent gauge boson masses are

$$m_W^2(\phi) = \frac{g^2}{2} (\phi_1^2 + \phi_2^2), \quad m_Z^2(\phi) = \frac{g^2 + g'^2}{2} (\phi_1^2 + \phi_2^2), \quad (18)$$

and the effective T -dependent masses of the longitudinal gauge bosons are

$$\overline{m}_{W_L}^2(\phi, T) = m_W^2(\phi) + \Pi_{W_L}(T), \quad (19)$$

$$\begin{aligned} \overline{m}_{Z_{L,\gamma_L}}^2(\phi, T) &= \frac{1}{2} \left[m_Z^2(\phi) + \Pi_{W_L}(T) + \Pi_{B_L}(T) \right] \\ &\pm \sqrt{\frac{1}{4} \left[\frac{g^2 - g'^2}{2} (\phi_1^2 + \phi_2^2) + \Pi_{W_L}(T) - \Pi_{B_L}(T) \right]^2 + \left[\frac{gg'}{2} (\phi_1^2 + \phi_2^2) \right]^2}. \end{aligned} \quad (20)$$

In eqs. (19) and (20), $\Pi_{W_L}(T)$ and $\Pi_{B_L}(T)$ are the leading parts of the T -dependent self-energies of W_L and B_L , given by

$$\Pi_{W_L}(T) = \frac{5}{2} g^2 T^2, \quad \Pi_{B_L}(T) = \frac{47}{18} g'^2 T^2, \quad (21)$$

where only loops of Higgs bosons, gauge bosons, Standard Model fermions and third-generation squarks have been included.

3. We shall now analyse the effective potential (1) as a function of ϕ and T . Before doing this, however, we trade the parameters m_1^2, m_2^2, m_3^2 appearing in the tree-level potential (2) for more convenient parameters. To this purpose, we first minimize the zero-temperature effective potential, i.e. we impose the vanishing of the first derivatives of $V_0(\phi) + V_1(\phi, 0)$ at $(\phi_1, \phi_2) = (v_1, v_2)$, where (v_1, v_2) are the one-loop vacuum expectation values at $T = 0$. This allows us to eliminate m_1^2 and m_2^2 in favour of m_Z^2 and $\tan \beta \equiv v_2/v_1$:

$$m_1^2 = -m_3^2 \tan \beta - \frac{m_Z^2}{2} \cos 2\beta - \sum_i \frac{n_i}{64\pi^2} \left[\frac{\partial m_i^2}{\partial \phi_1} \frac{m_i^2}{\phi_1} \left(\log \frac{m_i^2}{Q^2} - 1 \right) \right]_{\phi_{1,2}=v_{1,2}}, \quad (22)$$

$$m_2^2 = -m_3^2 \cot \beta + \frac{m_Z^2}{2} \cos 2\beta - \sum_i \frac{n_i}{64\pi^2} \left[\frac{\partial m_i^2}{\partial \phi_2} \frac{m_i^2}{\phi_2} \left(\log \frac{m_i^2}{Q^2} - 1 \right) \right]_{\phi_{1,2}=v_{1,2}}. \quad (23)$$

Moreover, m_3^2 can be traded for the one-loop-corrected mass m_A^2 of the CP-odd neutral Higgs boson. In our approximation [10]

$$m_3^2 = -m_A^2 \sin \beta \cos \beta - \frac{3g^2 m_t^2 \mu A_t}{32\pi^2 m_W^2 \sin^2 \beta} \frac{m_{\tilde{t}_1}^2 \left(\log \frac{m_{\tilde{t}_1}^2}{Q^2} - 1 \right) - m_{\tilde{t}_2}^2 \left(\log \frac{m_{\tilde{t}_2}^2}{Q^2} - 1 \right)}{m_{\tilde{t}_1}^2 - m_{\tilde{t}_2}^2}. \quad (24)$$

Therefore the whole effective potential (1) is completely determined, in our approximation, by the parameters $(m_A, \tan \beta)$ of the Higgs sector, and by the parameters $(m_t, m_{Q_3}, m_{U_3}, \mu, A_t)$ of the top/stop sector. The same set of parameters also determines the one-loop-corrected masses and couplings of the MSSM Higgs bosons.

The next steps are the computation of the critical temperature and of the location of the minimum of the effective potential at the critical temperature. We define here T_0 as the temperature at which the determinant of the second derivatives of $V_{\text{eff}}(\phi, T)$ at $\phi = 0$ vanishes:

$$\det \left[\frac{\partial^2 V_{\text{eff}}(\phi, T_0)}{\partial \phi_i \partial \phi_j} \right]_{\phi_{1,2}=0} = 0. \quad (25)$$

It is straightforward to compute the derivatives in eq. (25) from the previous formulae; the explicit expressions are

$$\begin{aligned} \frac{1}{2} \left[\frac{\partial^2 V_{\text{eff}}}{\partial \phi_i^2} \right]_0 &= m_i^2 + \frac{1}{64\pi^2} \left[6a_{ii} m_{Q_3}^2 \left(\log \frac{m_{Q_3}^2}{Q^2} - 1 \right) + 6b_{ii} m_{U_3}^2 \left(\log \frac{m_{U_3}^2}{Q^2} - 1 \right) \right] \\ &\quad + \frac{T^2}{4\pi^2} \left[\frac{\pi^2}{12} (9g^2 + 3g'^2 + \delta_{i2} \cdot 12h_t^2) + 6a_{ii} J'_+ \left(\frac{m_{Q_3}^2}{T^2} \right) + 6b_{ii} J'_+ \left(\frac{m_{U_3}^2}{T^2} \right) \right] \\ &\quad - \frac{T}{16\pi} \left\{ 3g^2 [\Pi_{W_L}(T)]^{\frac{1}{2}} + g'^2 [\Pi_{B_L}(T)]^{\frac{1}{2}} \right. \\ &\quad \left. + 6 \left[\bar{a}_{ii} (m_{Q_3}^2 + \Pi_{\tilde{t}_L}(T))^{\frac{1}{2}} - a_{ii} (m_{Q_3}^2)^{\frac{1}{2}} \right] \right\} \end{aligned}$$

$$\begin{aligned}
& + 6 \left[\bar{b}_{ii} \left(m_{U_3}^2 + \Pi_{\tilde{t}_R}(T) \right)^{\frac{1}{2}} - b_{ii} \left(m_{U_3}^2 \right)^{\frac{1}{2}} \right] \} , \\
\frac{1}{2} \left[\frac{\partial^2 V_{\text{eff}}}{\partial \phi_1 \partial \phi_2} \right]_0 &= m_3^2 + \frac{1}{64\pi^2} 6a_{12} \left[m_{Q_3}^2 \left(\log \frac{m_{Q_3}^2}{Q^2} - 1 \right) - m_{U_3}^2 \left(\log \frac{m_{U_3}^2}{Q^2} - 1 \right) \right] \\
& + \frac{T^2}{4\pi^2} 6a_{12} \left[J'_+ \left(\frac{m_{Q_3}^2}{T^2} \right) - J'_+ \left(\frac{m_{U_3}^2}{T^2} \right) \right] \\
& - \frac{T}{16\pi} \left\{ 6\bar{a}_{12} \left[\left(m_{Q_3}^2 + \Pi_{\tilde{t}_L}(T) \right)^{\frac{1}{2}} - \left(m_{U_3}^2 + \Pi_{\tilde{t}_R}(T) \right)^{\frac{1}{2}} \right] \right. \\
& \left. - 6a_{12} \left[\left(m_{Q_3}^2 \right)^{\frac{1}{2}} - \left(m_{U_3}^2 \right)^{\frac{1}{2}} \right] \right\} . \tag{26}
\end{aligned}$$

The coefficients a_{ij}, b_{ij} are given by

$$\begin{aligned}
a_{11} &\equiv \left(\frac{1}{2} - \frac{2}{3} \sin^2 \theta_W \right) (g^2 + g'^2) + \frac{2h_t^2 \mu^2}{m_{Q_3}^2 - m_{U_3}^2} , \\
b_{11} &\equiv \left(\frac{2}{3} \sin^2 \theta_W \right) (g^2 + g'^2) - \frac{2h_t^2 \mu^2}{m_{Q_3}^2 - m_{U_3}^2} , \\
a_{22} &\equiv 2h_t^2 - \left(\frac{1}{2} - \frac{2}{3} \sin^2 \theta_W \right) (g^2 + g'^2) + \frac{2h_t^2 A_t^2}{m_{Q_3}^2 - m_{U_3}^2} , \\
b_{22} &\equiv 2h_t^2 - \left(\frac{2}{3} \sin^2 \theta_W \right) (g^2 + g'^2) - \frac{2h_t^2 A_t^2}{m_{Q_3}^2 - m_{U_3}^2} , \\
a_{12} &\equiv \frac{2h_t^2 \mu A_t}{m_{Q_3}^2 - m_{U_3}^2} , \tag{27}
\end{aligned}$$

and the coefficients $\bar{a}_{ij}, \bar{b}_{ij}$ are given by identical expressions, apart from the replacement

$$m_{Q_3}^2 - m_{U_3}^2 \rightarrow m_{Q_3}^2 - m_{U_3}^2 + \Pi_{\tilde{t}_L}(T) - \Pi_{\tilde{t}_R}(T) . \tag{28}$$

Once eq. (25) is solved (numerically) and T_0 is found, one can minimize (numerically) the potential $V_{\text{eff}}(\phi, T_0)$ and find the minimum $[v_1(T_0), v_2(T_0)]$. The quantity of interest is indeed, as will be discussed later, the ratio $v(T_0)/T_0$, where $v(T_0) \equiv \sqrt{v_1^2(T_0) + v_2^2(T_0)}$.

4. Before moving to the discussion of our numerical results, we would like to present some approximate analytical formulae, which will be useful for a qualitative understanding of the various dependences of T_0 , $v_1(T_0)$ and $v_2(T_0)$. In this paragraph, we shall work in the limit of heavy degenerate stops, $m_{Q_3} = m_{U_3} \equiv \tilde{m} \gg T_0$ and $A_t = \mu = 0$, neglecting the D-term contributions to the stop squark masses, and keeping only the most important terms in the high-temperature expansions of the J_i functions for the gauge bosons and the top quark. In the chosen limit, the effective potential of eq. (1) can be approximately written, in the polar coordinates $\varphi \equiv \sqrt{\phi_1^2 + \phi_2^2}$ and $\tan \theta \equiv \phi_2/\phi_1$, as

$$V_{\text{eff}}(\phi, T) \simeq [a(\theta)T^2 - b(\theta)] \varphi^2 - ET\varphi^3 + \frac{1}{4}\lambda_T(\theta)\varphi^4 , \tag{29}$$

where

$$a(\theta) = \frac{3g^2 + g'^2}{16} + \frac{h_t^2}{4} \sin^2 \theta, \quad (30)$$

$$b(\theta) = \frac{m_Z^2}{2} \cos 2\beta \cos 2\theta - m_A^2 \sin^2(\beta - \theta) + \frac{3h_t^2}{8\pi^2} \sin^2 \theta m_t^2 \left(1 + \log \frac{\tilde{m}^2}{m_t^2} \right), \quad (31)$$

$$E = \frac{2\sqrt{2}}{3} \frac{1}{16\pi} \left[2g^3 + (g^2 + g'^2)^{3/2} \right], \quad (32)$$

$$\lambda_T(\theta) = \frac{1}{2}(g^2 + g'^2) \cos^2 2\theta + \frac{3h_t^4}{4\pi^2} \sin^4 \theta \left(\log \frac{\tilde{m}^2}{T^2} - 1.14 \right). \quad (33)$$

We have exploited the fact that, in the high-temperature limit, the terms proportional to $m_i^4 \log m_i^2$ cancel in the sum $V_1(\phi, 0) + \Delta V_1(\phi, T)$ (in the chosen limit, of course, we cannot perform the high-temperature expansion on the stop contributions).

We define the critical angle θ^* by the flat direction of the effective potential (1) around $\varphi = 0$ at $T = T_0$, and we denote by θ_{app}^* the analogous quantity evaluated from the approximate parametrization of eq. (29). The critical temperature T_0 and the critical angle θ_{app}^* are then determined by the conditions

$$\begin{cases} a(\theta_{\text{app}}^*) T_0^2 - b(\theta_{\text{app}}^*) = 0 \\ a'(\theta_{\text{app}}^*) T_0^2 - b'(\theta_{\text{app}}^*) = 0 \end{cases}. \quad (34)$$

Solving eq. (34) amounts to solving eq. (25) and finding the eigenvector corresponding to the zero eigenvalue. One finds

$$T_0^2 = \frac{-B + \sqrt{B^2 + AC}}{A}, \quad (35)$$

where

$$A = \frac{3g^2 + g'^2}{16} \frac{3g^2 + g'^2 + 4h_t^2}{16}, \quad (36)$$

$$\begin{aligned} B = & \frac{3g^2 + g'^2 + 2h_t^2(1 - \cos 2\beta)}{32} m_A^2 - \frac{h_t^2}{16} \cos 2\beta m_Z^2 \\ & - \frac{3g^2 + g'^2}{16} \frac{3h_t^2}{16\pi^2} m_t^2 \left(1 + \log \frac{\tilde{m}^2}{m_t^2} \right), \end{aligned} \quad (37)$$

$$\begin{aligned} C = & \left[m_Z^2 \cos^2 2\beta + (1 - \cos 2\beta) \frac{3h_t^2}{8\pi^2} m_t^2 \left(1 + \log \frac{\tilde{m}^2}{m_t^2} \right) \right] \frac{m_A^2}{2} \\ & + \left[\frac{m_Z^2}{2} \cos^2 2\beta - \cos 2\beta \frac{3h_t^2}{8\pi^2} m_t^2 \left(1 + \log \frac{\tilde{m}^2}{m_t^2} \right) \right] \frac{m_Z^2}{2}, \end{aligned} \quad (38)$$

and

$$\tan 2\theta_{\text{app}}^* = \tan 2\beta \frac{m_A^2}{m_A^2 + m_Z^2 + \left[\frac{h_t^2 T_0^2}{4} - \frac{3h_t^2}{8\pi^2} m_t^2 \left(1 + \log \frac{\tilde{m}^2}{m_t^2} \right) \right] / \cos 2\beta}, \quad (39)$$

where T_0 is determined by eq. (35). If we now assume that $\tan \theta(T_0) \equiv v_2(T_0)/v_1(T_0)$ can be approximated by $\tan \theta_{\text{app}}^*$, we can also write

$$\left[\frac{v(T_0)}{T_0} \right]_{\text{app}} \simeq \frac{3E}{\lambda_{T_0}(\theta_{\text{app}}^*)}. \quad (40)$$

In fig. 1, we plot $\tan \theta(T_0)$ (solid lines) and $\tan \theta^*$ (dashed lines) as functions of m_A , for $\tan \beta = 1, 2, 5$ and the representative parameter choice $m_t = 150$ GeV, $m_{Q_3} = m_{U_3} = 1$ TeV, $A_t = \mu = 0$. We can see that, in all cases, $\tan \theta(T_0) \simeq \tan \theta^*$ to a very good accuracy. To check our analytical approximation, we also plot $\tan \theta_{\text{app}}^*$ (dotted lines) as obtained from eq. (39). We can see from fig. 1 that all three quantities tend to the corresponding value of $\tan \beta$ for large values of m_A , whereas they increase to large values for small values of m_A . This fact is a general trend of V_{eff} , for arbitrary values of the top/stop parameters. As for $v(T_0)/T_0$, we have also checked that the analytical expression (40) is an adequate approximation to the numerical value obtained from (1) and (25). The qualitative behaviour of $v(T_0)/T_0$ can then be derived from (40), (33), (35) and (39): for fixed m_A , $v(T_0)/T_0$ increases when $\tan \beta$ is approaching 1 from above; for fixed $\tan \beta$, $v(T_0)/T_0$ is an increasing function of m_A .

5. We now discuss the particle physics constraints on the parameters of the top/stop sector and of the Higgs sector. To be as general as possible, we treat m_{Q_3} , m_{U_3} and the other soft mass terms as independent parameters, even if they can be related in specific supergravity models.

The constraints on the top/stop sector have already been discussed in [7], so we just recall them briefly. Direct and indirect searches at LEP [4] imply that $m_{\tilde{b}_L} \gtrsim 45$ GeV, which in turn translates into a bound in the $(m_{Q_3}, \tan \beta)$ plane. Electroweak precision measurements [11] put stringent constraints on a light stop-sbottom sector: in first approximation, and taking into account possible effects [12] of other light particles of the MSSM, we conservatively summarize the constraints by $\Delta\rho(t, b) + \Delta\rho(\tilde{t}, \tilde{b}) < 0.01$, where the explicit expression for $\Delta\rho(\tilde{t}, \tilde{b})$ can be found in [13].

We finally need to consider the constraints coming from LEP searches for supersymmetric Higgs bosons [4]. Experimentalists put limits on the processes $Z \rightarrow hZ^*$ and $Z \rightarrow hA$, where h is the lighter neutral CP-even boson. We need to translate these limits into exclusion contours in the $(m_A, \tan \beta)$ plane, for given values of the top/stop parameters. In order to do this, we identify the value of $BR(Z \rightarrow hZ^*)$, which corresponds to the limit $m_\phi > 63.5$ GeV on the SM Higgs, and the value of $BR(Z \rightarrow hA)$, which best fits the published limits for the representative parameter choice $m_t = 140$ GeV, $m_{Q_3} = m_{U_3} \equiv \tilde{m} = 1$ TeV, $A_t = \mu = 0$. We then compare those values of $BR(Z \rightarrow hZ^*)$ and $BR(Z \rightarrow hA)$ with the theoretical predictions of the MSSM, for any desired parameter choice and after including the radiative corrections associated to top/stop loops [14,10]. Of course, this procedure is not entirely correct, since it ignores the variations of the ef-

ficiencies with the Higgs masses and branching ratios, as well as the possible presence of candidate events at some mass values, but it is adequate for our purposes.

6. We now present our numerical results, based on the effective potential of eq. (1), concerning the strength of the electroweak phase transition and the condition for preserving the baryon asymmetry. According to [15], the condition to avoid erasing any previously generated baryon asymmetry via sphaleron transitions is

$$\frac{E_{sph}(T_C)}{T_C} > 45, \quad (41)$$

where T_C is the actual temperature at which the phase transition occurs, satisfying the inequalities

$$T_0 < T_C < T_D, \quad (42)$$

if T_0 is defined by (25) and T_D is the temperature at which there are two degenerate minima. Particularizing to the MSSM the studies of sphalerons in general two-Higgs models [16], we obtain that

$$E_{sph}^{MSSM}(T) \leq E_{sph}^{SM}(T), \quad (43)$$

where, in our conventions,

$$\frac{E_{sph}^{SM}(T)}{T} = \frac{4\sqrt{2}\pi}{g} B \left\{ \frac{\lambda_{\text{eff}}[\theta(T)]}{4g^2} \right\} \frac{v(T)}{T}, \quad (44)$$

and B is a smoothly varying function whose values can be found in [17]. For example, $B(10^{-2}) = 1.67$, $B(10^{-1}) = 1.83$, $B(1) = 2.10$. It can also be shown that

$$\frac{v(T_D)}{T_D} < \frac{v(T_C)}{T_C} < \frac{v(T_0)}{T_0}. \quad (45)$$

Finally, the corrections in E_{sph}^{SM} due to $g' \neq 0$ have been estimated and shown to be small [18]. Therefore, a conservative bound to be imposed is

$$R \equiv \frac{v(T_0)}{T_0} \frac{4\sqrt{2}\pi B \left\{ \frac{\lambda_{\text{eff}}[\theta(T_0)]}{4g^2} \right\}}{45g} > 1. \quad (46)$$

The last point to be discussed is the determination of the value of $\lambda_{\text{eff}}[\theta(T_0)]$ to be plugged into eq. (46). The B -function we use is taken from ref. [17], where the sphaleron energy was computed using the zero-temperature ‘Mexican-hat’ potential, $V = \frac{\lambda}{4}(\phi^2 - v^2)^2$. The sphaleron energy at finite temperature was computed in ref. [19], where it was proven that it scales like $v(T)$, i.e.

$$E_{sph}^{SM}(T) = E_{sph}^{SM}(0) \frac{v(T)}{v}, \quad (47)$$

with great accuracy. Therefore, to determine the value of $\lambda_{\text{eff}}[\theta(T_0)]$ we have fitted $V_{\text{eff}}(\phi, T_0)$, as given by eq. (1), to the appropriate approximate expression,

$$V_{\text{eff}}(\phi, T_0) \simeq \frac{1}{4} \lambda_{\text{eff}}[\theta(T_0)] [\phi^2 - v^2(T_0)]^2 + \text{field-independent terms}, \quad (48)$$

where the field-independent terms are just to take care of the different normalizations of the left- and right-hand sides. The value of λ_{eff} obtained from (48),

$$\lambda_{\text{eff}}[\theta(T_0)] = 4 \frac{V_{\text{eff}}(0, T_0) - V_{\text{eff}}[v(T_0), T_0]}{v^4(T_0)}, \quad (49)$$

where all quantities on the right-hand side are calculated numerically from the potential of eq. (1), is then plugged into eq. (46) to obtain our bounds. We have explicitly checked the quality of the fit in eq. (48), finding an agreement that is more than adequate for our purposes.

Our numerical results are summarized in fig. 2, in the $(m_A, \tan \beta)$ plane and for two representative values of the top quark mass: $m_t = 130$ GeV (fig. 2a) and $m_t = 170$ GeV (fig. 2b). In each case, the values of the remaining free parameters have been chosen in order to maximize the strength of the phase transition, given the experimental constraints on the top-stop sector. Notice that arbitrarily small values of m_{U_3} cannot be excluded on general grounds, even if they are disfavoured by model calculations. Also, we have explicitly checked that, as in ref. [7], mixing effects in the stop mass matrix always worsen the case. In fig. 2, solid lines correspond to contours of constant R : one can see that the requirement of large values of R favours small $\tan \beta$ and $m_A \gg m_Z$. The thick solid line corresponds to the limits coming from Higgs searches at LEP: for our parameter choices, the allowed regions correspond to large $\tan \beta$ and/or $m_A \gg m_Z$. For reference, contours of constant m_h (in GeV) have also been plotted as dashed lines. One can see that, even for third-generation squarks as light as allowed by all phenomenological constraints, only a very small globally allowed region can exist in the $(m_A, \tan \beta)$ plane, and that the most favourable situation is the one already discussed in ref. [7]. More precisely, the region that is still marginally allowed corresponds to $m_A \gg m_Z$, $\tan \beta \sim 2$, stop and sbottom sectors as light as otherwise allowed, a heavy top, and a light Higgs boson with SM-like properties and mass $m_h \sim 65$ GeV, just above the present experimental limit. A less conservative interpretation of the limits from precision measurements, the inclusion of some theoretically motivated constraints on the model parameters, or a few GeV improvement in the SM Higgs mass limit, would each be enough to fully exclude electroweak baryogenesis in the MSSM.

7. In summary, our analysis of the full $(m_A, \tan \beta)$ parameter space extends and confirms the results of ref. [7]: in the region of the MSSM parameter space allowed by the present experimental constraints, there is very little room for fulfilling the constraint

(46), which is a necessary condition for electroweak baryogenesis. To put these results in a clearer perspective, some final comments on possible ways out are in order.

First, one could think of relaxing the constraint $\tan \beta \geq 1$ (and the corresponding LEP bounds), which is usually motivated by the theoretical assumption of universal soft Higgs masses at the SUSY-GUT scale, $M_U \sim 10^{16}$ GeV. The possibility of $\tan \beta < 1$, however, is incompatible with a heavy top quark, since, for $m_t \gtrsim 130$ GeV and supersymmetric particle masses of order m_Z , the running top Yukawa coupling would become non-perturbative at scales smaller than M_U : such a possibility is strongly disfavoured by the successful predictions of the low-energy gauge couplings in SUSY GUTs.

A second possibility is that large non-perturbative effects, neglected by conventional calculational techniques, modify the predicted values of the sphaleron energy and/or of $v(T_0)/T_0$ (for recent suggestions along this line, see [20]). We do not see strong physical arguments to favour this, but we admit that it cannot be rigorously excluded. Perhaps alternative approaches to the electroweak phase transition [21] could help clarify this point in the future.

Barring the above-mentioned possibilities, one could still try to rescue electroweak baryogenesis by further enlarging the MSSM Higgs sector, for example by introducing an extra singlet. Supersymmetric models with singlets and non-supersymmetric models, however, develop dangerous instabilities if coupled to the superheavy sector of an underlying unified theory. It might well be that baryogenesis has to be described by physics at a scale larger than the electroweak one.

Acknowledgements

We would like to thank J.-F. Grivaz for helping us to understand the LEP limits on the MSSM Higgs bosons. One of us (F.Z.) would like to thank IEM-CSIC for the warm hospitality during the final phase of this work. Another of us (J.R.E.) wants to thank the SCIPP for the warm hospitality during part of this work.

References

1. For reviews and references see, e.g.:
M.E. Shaposhnikov, in ‘Proceedings of the 1991 Summer School in High Energy Physics and Cosmology’, Trieste, 17 June–9 August 1991, E. Gava et al., eds. (World Scientific, Singapore, 1992), Vol. 1, p. 338;
A.D. Dolgov, *Phys. Rep.* 222 (1992) 309;
A.G. Cohen, D.B. Kaplan and A.E. Nelson, *Ann. Rev. Nucl. Part. Sci.* 43 (1993) 27.
2. G. Farrar and M.E. Shaposhnikov, *Phys. Rev. Lett.* 70 (1993) 2833 + (E) 71 (1993) 210 and preprint CERN-TH.6734/93.
3. M.B. Gavela, P. Hernández, J. Orloff and O. Pène, preprint CERN-TH.7081/93.
4. See, e.g.: G. Coignet, Plenary talk at the XVI International Symposium on Lepton-Photon Interactions, Cornell University, Ithaca, New York, 10–15 August 1993, to appear in the Proceedings, and references therein.
5. M.E. Carrington, *Phys. Rev.* D45 (1992) 2933;
M. Dine, R.G. Leigh, P. Huet, A. Linde and D. Linde, *Phys. Lett.* B283 (1992) 319 and *Phys. Rev.* D46 (1992) 550;
P. Arnold, *Phys. Rev.* D46 (1992) 2628;
J.R. Espinosa, M. Quirós and F. Zwirner, *Phys. Lett.* B314 (1993) 206;
P. Arnold and O. Espinosa, *Phys. Rev.* D47 (1993) 3546;
W. Buchmüller, Z. Fodor, T. Helbig and D. Walliser, preprint DESY 93-021.
6. A.G. Cohen and A.E. Nelson, *Phys. Lett.* B297 (1992) 111.
7. J.R. Espinosa, M. Quirós and F. Zwirner, *Phys. Lett.* B307 (1993) 106.
8. G.F. Giudice, *Phys. Rev.* D45 (1992) 3177;
S. Myint, *Phys. Lett.* B287 (1992) 325.
9. D. Comelli and M. Pietroni, *Phys. Lett.* B306 (1993) 67;
J.R. Espinosa, J.M. Moreno and M. Quirós, Madrid preprint IEM-FT-76/93, to appear in *Physics Letters B* (1993).
10. J. Ellis, G. Ridolfi and F. Zwirner, *Phys. Lett.* B262 (1991) 477.
11. See, e.g.: G. Altarelli, Plenary talk given at the International Europhysics Conference on High Energy Physics, Marseille, 22–28 July 1993, preprint CERN-TH.7045/93, to appear in the Proceedings, and references therein.

12. R. Barbieri, M. Frigeni and F. Caravaglios, *Phys. Lett.* B279 (1992) 169;
 G. Altarelli, R. Barbieri and F. Caravaglios, *Nucl. Phys.* B405 (1993) 3, preprint
 CERN-TH.6859/93 and *Phys. Lett.* B314 (1993) 357;
 J. Ellis, G.L. Fogli and E. Lisi, *Phys. Lett.* B285 (1992) 238, B286 (1992) 85 and
Nucl. Phys. B393 (1993) 3.
13. L. Alvarez-Gaumé, J. Polchinski and M. Wise, *Nucl. Phys.* B221 (1983) 495;
 R. Barbieri and L. Maiani, *Nucl. Phys.* B224 (1983) 32;
 C.S. Lim, T. Inami and N. Sakai, *Phys. Rev.* D29 (1984) 1488.
14. Y. Okada, M. Yamaguchi and T. Yanagida, *Prog. Theor. Phys.* Lett. 85 (1991) 1
 and *Phys. Lett.* B262 (1991) 54;
 J. Ellis, G. Ridolfi and F. Zwirner, *Phys. Lett.* B257 (1991) 83;
 H.E. Haber and R. Hempfling, *Phys. Rev. Lett.* 66 (1991) 1815;
 R. Barbieri and M. Frigeni, *Phys. Lett.* B258 (1991) 395.
15. M. Shaposhnikov, *JETP Lett.* 44 (1986) 465; *Nucl. Phys.* B287 (1987) 757 and
 B299 (1988) 797.
16. A. Bochkarev, S. Kuzmin and M. Shaposhnikov, *Phys. Rev.* D43 (1991) 369 and
Phys. Lett. B244 (1990) 275;
 B. Kastening, R.D. Peccei and X. Zhang, *Phys. Lett.* B266 (1991) 413.
17. F.R. Klinkhamer and N.S. Manton, *Phys. Rev.* D30 (1984) 2212.
18. J. Kunz, B. Kleihaus and Y. Brihaye, *Phys. Rev.* D46 (1992) 3587.
19. S. Braibant, Y. Brihaye and J. Kunz, Utrecht preprint THU-93/01.
20. K. Kajantie, K. Rummukainen and M. Shaposhnikov, *Nucl. Phys.* B407 (1993) 356;
 M. Shaposhnikov, *Phys. Lett.* B316 (1993) 112.
21. B. Bunk, E.M. Ilgenfritz, J. Kripfganz and A. Schiller, *Phys. Lett.* B284 (1992) 371
 and *Nucl. Phys.* B403 (1993) 453;
 J. March-Russell, *Phys. Lett.* B296 (1992) 364;
 H. Meyer-Ortmanns and A. Patkós, *Phys. Lett.* B297 (1993) 331;
 A. Jakováć and A. Patkós, *Z. Phys.* C60 (1993) 361;
 N. Tetradis and C. Wetterich, *Nucl. Phys.* B398 (1993) 659 and preprint DESY-93-
 128;
 P. Arnold and L.G. Yaffe, University of Washington preprint UW/PT-93-24.

Figure captions

Fig.1: The quantities $\tan \theta(T_0)$ (solid lines), $\tan \theta^*$ (dashed lines) and $\tan \theta_{\text{app}}^*$ (dotted lines), as functions of m_A , for $\tan \beta = 1, 2, 5$ and the representative parameter choice $m_t = 150$ GeV, $m_{Q_3} = m_{U_3} = 1$ TeV, $A_t = \mu = 0$.

Fig.2: Contours of R in the $(m_A, \tan \beta)$ plane, for the parameter choices: a) $m_t = 130$ GeV, $m_{Q_3} = 50$ GeV, $m_{U_3} = 0$ ($m_{\tilde{t}} \sim 130$ GeV, $m_{\tilde{b}_L} \sim 50$ GeV), $A_t = \mu = 0$; b) $m_t = 170$ GeV, $m_{Q_3} = 280$ GeV, $m_{U_3} = 0$ ($m_{\tilde{t}_L} \sim 330$ GeV, $m_{\tilde{t}_R} \sim 170$ GeV, $m_{\tilde{b}_L} \sim 280$ GeV), $A_t = \mu = 0$. The region excluded by Higgs searches at LEP is delimited by the thick solid line. For reference, contours of constant m_h (in GeV) are also represented as dashed lines.

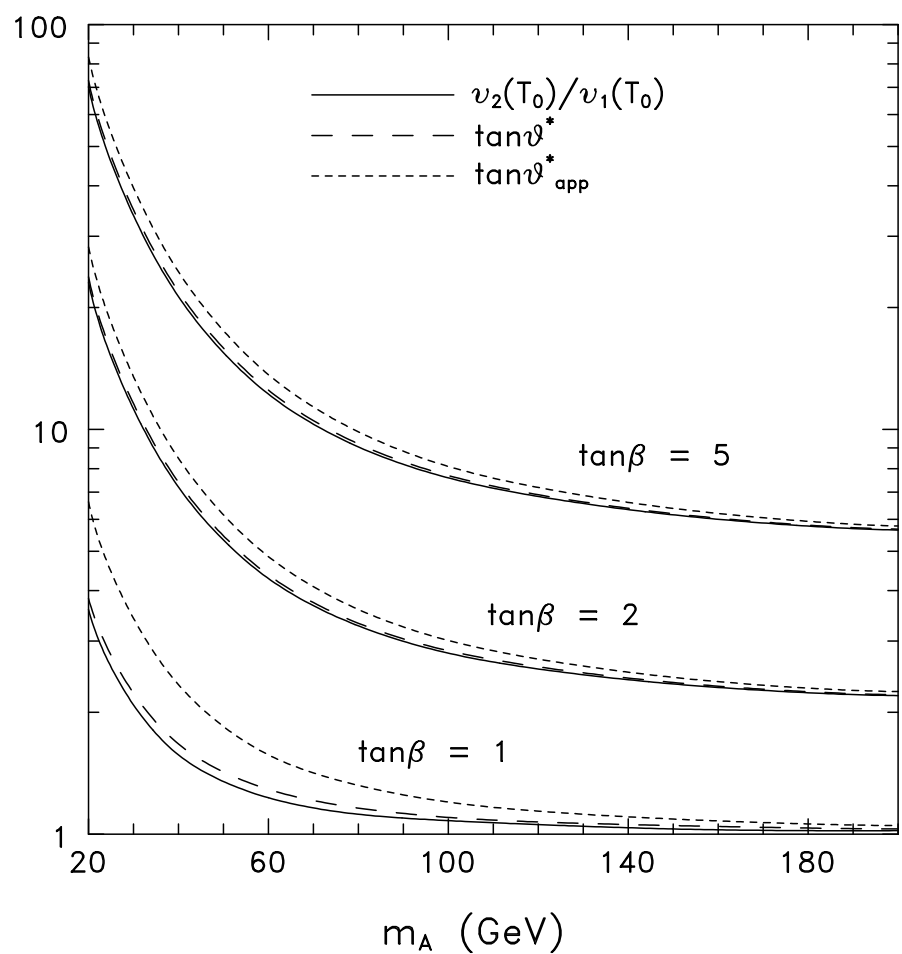


Fig. 1

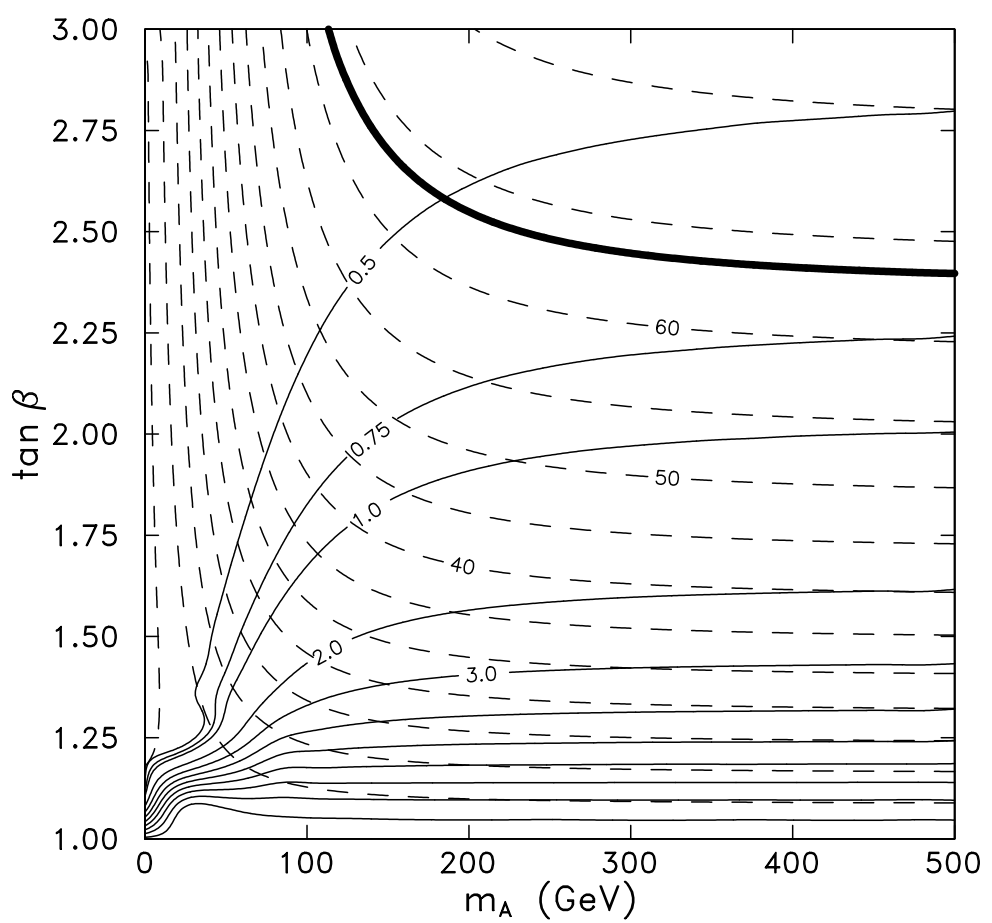


Fig. 2a

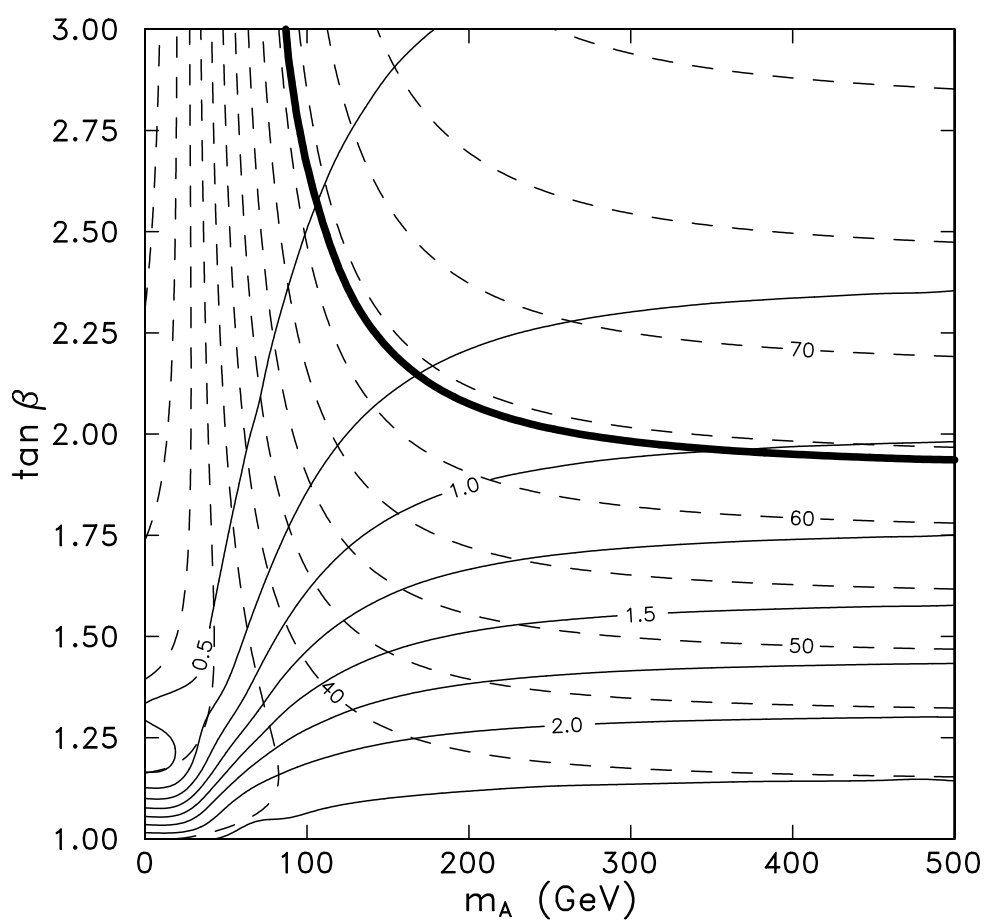


Fig. 2b